An integrated solution and analysis of bioluminescence tomography and diffuse optical tomography

Weimin Han[1,*,†], Wenxiang Cong[2], Kamran Kazmi[1] and Ge Wang[2]

[1]*Department of Mathematics, University of Iowa, Iowa City, IA 52242, U.S.A.*
[2]*Division of Biomedical Imaging, Virginia Tech-Wake Forest, University School of Biomedical Engineering and Sciences, Virginia Polytechnic Institute and State University, Blacksburg, VA 24061, U.S.A.*

SUMMARY

While diffuse optical tomography (DOT) has been studied for years, bioluminescence tomography (BLT) is emerging as a promising optical molecular imaging tool. These two modalities have different goals. DOT is for reconstruction of optical parameters of a medium such as a breast from surface measurements induced by external sources. BLT is for reconstruction of a bioluminescent source distribution in a medium such as a mouse from surface measurements induced by internal bioluminescent sources. However, an important pre-requisite for BLT reconstruction is the knowledge on the distribution of optical parameters within the medium, which is the output of DOT. In this paper, we propose a mathematical model integrating BLT and DOT at the fundamental level; that is, performing the two types of reconstructions simultaneously instead of doing them sequentially. The model is introduced through minimizing the difference between predicted quantities and boundary measurements, as well as incorporating regularization terms. Then, we show the solution existence, introduce numerical schemes and prove convergence of the numerical solution. We also present numerical results to illustrate the utility of our approach. Copyright © 2008 John Wiley & Sons, Ltd.

1. INTRODUCTION

Roughly speaking, the biomedical imaging technology is characterized by the traditional anatomical imaging modes such as X-ray computed tomography (CT), the popular functional imaging

*Correspondence to: Weimin Han, Department of Mathematics, University of Iowa, Iowa City, IA 52242, U.S.A.
†E-mail: whan@math.uiowa.edu

modes such as functional magnetic resonance imaging (MRI), and the futuristic molecular imaging modes such as various types of optical molecular imaging techniques. Bioluminescence tomography (BLT), which we have been developing since 2002, is an emerging optical molecular imaging tool. As compared with fluorescence-based imaging, bioluminescence imaging does not suffer from background auto-fluorescence and has unique probing capabilities. With BLT, 3D localization and quantitative analyses on a bioluminescent source distribution may be performed in mouse models, which are important to study human disease progression and therapeutic efficacy.

Currently, results from our and other groups all suggest that BLT does produce valuable tomographic information in cases of favorable source locations or with *a priori* knowledge. In an important type of these cases, the distribution of optical parameters within a mouse is known, which can be determined using diffuse optical tomography (DOT). Nevertheless, the DOT solution is not accurate in general, and it is not always reliable either. In brief, it remains extremely challenging to stabilize the BLT reconstruction and reduce its errors significantly.

In this paper, we develop the first mathematical model that allows the simultaneous reconstruction of both optical parameters and bioluminescent source distributions within the mouse. The physical experiment starts with applying several sets of external laser beams of appropriate wavelengths on the mouse body surface to excite the biological medium, and subsequently collect photon densities with charge-coupled device (CCD) detectors on certain parts of the boundary. Then, the substrate is administrated into the blood circulation of the mouse to generate bioluminescent photons, and the corresponding signals are similarly recorded on the mouse body surface. For the mathematical model to be introduced next, we assume that the experiment is done in a totally dark environment. Nevertheless, this assumption is neither essential for analysis of the model nor for its implementation.

We proceed to describe the mathematical model in its classical formulation. To simplify the notation, we use the subscript D for quantities related to the DOT part and the subscript B for the BLT part. We also assume that all spaces related to DOT part are complex valued and the ones related to BLT part are real valued.

Let $\Omega \subset \mathbb{R}^d$ be the biological medium with the boundary $\Gamma = \partial \Omega$. Although the dimension $d = 3$ for applications, the theory we develop is valid for any dimension. Suppose a total of I sets of measurement data are available for the DOT part. We denote by $\Gamma_{D,i}$, $1 \leqslant i \leqslant I$, subsets of Γ where DOT measurement data are collected. We denote by Γ_B the part of the boundary where the BLT measurement data are collected. Note that these boundary subsets are allowed to be the entire boundary. Given sources $p_{D,i}$ on Γ, modified measurements $g_{D,i}$ on $\Gamma_{D,i}$, permissible region $\Omega_B \subset \Omega$, and modified measurement g_B on Γ_B, we need to determine the optical parameters κ, μ and the source function p such that for $i = 1, \ldots, I$, the solution $u_{D,i}$ of the boundary value problem (BVP)

$$-\text{div}(\kappa \nabla u_{D,i}) + \mu u_{D,i} + \frac{i\omega}{c_0} u_{D,i} = 0 \quad \text{in } \Omega \tag{1}$$

$$u_{D,i} + 2A\kappa \frac{\partial u_{D,i}}{\partial \nu} = p_{D,i} \quad \text{on } \Gamma \tag{2}$$

satisfies

$$u_{D,i} = g_{D,i} \quad \text{on } \Gamma_{D,i} \tag{3}$$

and the solution u_B of the BVP

$$-\text{div}(\kappa \nabla u_B) + \mu u_B = p\chi_B \quad \text{in } \Omega \tag{4}$$

$$u_B + 2A\kappa \frac{\partial u_B}{\partial v} = 0 \quad \text{on } \Gamma \tag{5}$$

satisfies

$$u_B = g_B \quad \text{on } \Gamma_B \tag{6}$$

In (1), c_0 denotes the light speed and ω is the modulation frequency. In (4), we use the notation χ_B for the characteristic function of the set Ω_B. The parameter $\kappa = 1/[3(\mu + \mu')]$, μ and μ' being absorption and reduced scattering coefficients. We use $\partial/\partial v$ to denote the operator of outward normal differentiation. The appearance of the parameter A in the boundary condition (2) and (5) is to incorporate diffuse boundary reflection arising from a refractive index mismatch between the body Ω and the surrounding medium.

A conventional DOT problem is to determine the optical parameters κ and μ from (1)–(3). A summary account of DOT can be found in [1]. In the conventional BLT problem, the parameters κ and μ are assumed to be known exactly, and the only unknown is the source function p. Theoretical studies of the BLT problem have been done in [2, 3], and that of multispectral bioluminescence tomography are found in [4, 5]. We note that in the conventional BLT, since the parameters κ and μ are determined from separate experiments of DOT, these parameters are known only approximately. In this paper, we propose a new approach that combines DOT and BLT together so as to reconstruct the optical parameters and the bioluminescent source distribution simultaneously. In Section 2, we formulate the problem of simultaneous reconstruction of both the bioluminescent source distribution and the optical parameters, and then prove the solution existence. In Section 3, we discuss numerical approximations and the convergence of numerical methods. In Section 4, we present numerical examples to illustrate the utility of our approach and evaluate its performance.

2. FORMULATION AND THEORETICAL INVESTIGATION

To formulate the problem rigorously, we need to make some assumptions on the given data. We assume $\Omega \subset \mathbb{R}^d$ is a non-empty, open, bounded set with a Lipschitz boundary Γ, and $\Gamma_{D,i}$, $1 \leqslant i \leqslant m$, and Γ_B are Lipschitz subsets of Γ. The parameter A is assumed to be bounded and bounded below away from zero. We also assume $g_{D,i} \in L^2(\Gamma_{D,i})$, $1 \leqslant i \leqslant I$, and $g_B \in L^2(\Gamma_B)$. Note that $L^2(\Gamma_{D,i})$, $1 \leqslant i \leqslant I$, are complex valued and $L^2(\Gamma_B)$ is a real Hilbert space. In this paper, function spaces with a subscript D are complex, whereas those with a subscript B are real.

In most applications of DOT and BLT, the parameters κ and μ are taken to be piecewise constants. In other words, the biological medium $\overline{\Omega}$ consists of J subdomains $\overline{\Omega_j}$, $1 \leqslant j \leqslant J$, such that $\overline{\Omega} = \bigcup_{j=1}^{J} \overline{\Omega_j}$, $\Omega_j \cap \Omega_l = \emptyset$ for $j \neq l$, and restrictions of κ and μ on each Ω_j are constants. To allow a framework for more accurate identification of the parameters, we consider a general situation where the restriction of κ to each Ω_j belongs to a finite-dimensional function space, and μ belongs to a general convex, closed set in the real space $L^2(\Omega)$. Thus, over each Ω_j, we

introduce a finite-dimensional function space $X_j \subset L^\infty(\Omega_j)$. For given constants $\underline{\kappa}_j, \overline{\kappa}_j \in (0, \infty)$, $1 \leqslant j \leqslant J$, let

$$Q_\kappa = \{\kappa \in L^\infty(\Omega) \,|\, \underline{\kappa}_j \leqslant \kappa \leqslant \overline{\kappa}_j \text{ a.e. in } \Omega_j, \ \kappa|_{\Omega_j} \in X_j, \ 1 \leqslant j \leqslant J\} \tag{7}$$

be the set where we look for the parameter κ. For given constants $\underline{\mu}_j \geqslant 0$ and $\overline{\mu}_j > 0$, $1 \leqslant j \leqslant J$, let

$$Q_\mu \subset \{\mu \in L^2(\Omega) \,|\, \underline{\mu}_j \leqslant \mu \leqslant \overline{\mu}_j \text{ a.e. in } \Omega_j, \ 1 \leqslant j \leqslant J\} \tag{8}$$

be a closed, convex set of $L^2(\Omega)$. The constants $\underline{\kappa}_j$, $\overline{\kappa}_j$, $\underline{\mu}_j$, and $\overline{\mu}_j$, $1 \leqslant j \leqslant J$, are selected based on experimental results. In practice, X_j is chosen to be the constant function space on Ω_j, and similarly, Q_μ is a set of piecewise constant functions.

Suppose, we seek the source function p in a closed convex subset Q_p of the real Hilbert space $L^2(\Omega_B)$:

$$Q_p \subset \{p \in L^2(\Omega_B) \,|\, p \geqslant 0 \text{ a.e. in } \Omega_B\} \tag{9}$$

For example, Q_p may be chosen as a set of non-negatively valued functions from a finite-dimensional space of linear combinations of specified functions such as the characteristic functions of certain subsets of Ω_B.

We then define the admissible set $Q_{\text{ad}} = Q_\kappa \times Q_\mu \times Q_p$. Also we denote by V_D and Q_D the complex Hilbert spaces $H^1(\Omega)$ and $L^2(\Gamma)$, respectively, and by V_B and Q_B the real spaces $H^1(\Omega)$ and $L^2(\Gamma)$, respectively.

For any $(\kappa, \mu) \in Q_\kappa \times Q_\mu$, define $u_{D,i} = u_{D,i}(\kappa, \mu) \in V_D$ by the BVP

$$\int_\Omega \left[\kappa \nabla u_{D,i} \cdot \nabla \bar{v} + \left(\mu + \frac{\mathrm{i}\omega}{c_0} \right) u_{D,i} \bar{v} \right] \mathrm{d}x + \int_\Gamma \frac{1}{2A} u_{D,i} \bar{v} \, \mathrm{d}s = \int_\Gamma \frac{1}{2A} p_{D,i} \bar{v} \, \mathrm{d}s \quad \forall v \in V_D \tag{10}$$

Additionally, with any $p \in L^2(\Omega_B)$, denote $u_B = u_B(\kappa, \mu, p) \in V_B$ the solution of the BVP

$$\int_\Omega (\kappa \nabla u_B \cdot \nabla v + \mu u_B v) \, \mathrm{d}x + \int_\Gamma \frac{1}{2A} u_B v \, \mathrm{d}s = \int_{\Omega_B} p \, v \, \mathrm{d}x \quad \forall v \in V_B \tag{11}$$

Then the weak solution of the problem (1)–(2) is $u_{D,i} = u_{D,i}(\kappa, \mu)$, and that of (4)–(5) is $u_B = u_B(\kappa, \mu, p)$. By the well-known Lax–Milgram Lemma (e.g. [6, 7]) and its complex version (e.g. [8]), due to the assumptions made on the data, the problems (10) and (11) have a unique solution.

For $\varepsilon_\kappa \geqslant 0$, $\varepsilon_\mu \geqslant 0$ and $\varepsilon_p \geqslant 0$, denote $\varepsilon = (\varepsilon_\kappa, \varepsilon_\mu, \varepsilon_p)$, and define the functional

$$J_\varepsilon(\kappa, \mu, p) = \frac{1}{2} \sum_{i=1}^I \|u_{D,i}(\kappa, \mu) - g_{D,i}\|_{L^2(\Gamma_{D,i})}^2 + \frac{1}{2} \|u_B(\kappa, \mu, p) - g_B\|_{L^2(\Gamma_B)}^2$$

$$+ \frac{\varepsilon_\kappa}{2} \|\kappa\|_{L^2(\Omega)}^2 + \frac{\varepsilon_\mu}{2} \|\mu\|_{L^2(\Omega)}^2 + \frac{\varepsilon_p}{2} \|p\|_{L^2(\Omega_B)}^2 \tag{12}$$

We introduce the following problem for simultaneous determination of the parameters κ and μ, and the source function p:

$$\inf\{J_\varepsilon(\kappa, \mu, p) \,|\, (\kappa, \mu, p) \in Q_{\text{ad}}\} \tag{13}$$

First, we address the solution existence.

Theorem 2.1
Assume $\varepsilon_p > 0$ or $Q_p \subset L^2(\Omega_B)$ is bounded. Then the problem (13) has a solution.

Proof
Denote by $\alpha \geqslant 0$ the infimum value of (13). By the definition of infimum, there is a sequence $\{(\kappa_n, \mu_n, p_n)\}_{n \geqslant 1} \subset Q_{\mathrm{ad}}$ such that

$$J_\varepsilon(\kappa_n, \mu_n, p_n) \to \alpha \quad \text{as } n \to \infty$$

Denote $u_{D,i,n} = u_{D,i}(\kappa_n, \mu_n)$, $u_{B,n} = u_B(\kappa_n, \mu_n, p_n)$. Then it is easy to see that the sequences $\{\|u_{D,i,n}\|_{V_D}\}$ and $\{\|u_{B,n}\|_{V_B}\}$ are bounded. Under the assumption that $\varepsilon_p > 0$ or $Q_p \subset L^2(\Omega_B)$ is bounded, $\{p_n\}$ is a bounded sequence in $L^2(\Omega_B)$. Since Q_κ is finite dimensional and $\{\|\mu_n\|_{L^2(\Omega)}\}$ is bounded, we can find a subsequence $\{n'\}$ of the sequence $\{n\}$, and some functions $\kappa_\infty \in Q_\kappa$, $\mu_\infty \in Q_\mu$, $p_\infty \in Q_p$, $u_{D,i,\infty} \in V_D$, and $u_{B,\infty} \in V_B$ such that as $n' \to \infty$

$$\kappa_{n'} \to \kappa_\infty \quad \text{in } L^\infty(\Omega), \quad \mu_{n'} \rightharpoonup \mu_\infty \quad \text{in } L^2(\Omega), \quad p_{n'} \rightharpoonup p_\infty \quad \text{in } L^2(\Omega_B)$$

$$u_{D,i,n'} \rightharpoonup u_{D,i,\infty} \quad \text{in } V_D, \quad u_{B,n'} \rightharpoonup u_{B,\infty} \quad \text{in } V_B$$

$$u_{D,i,n'} \to u_{D,i,\infty} \quad \text{in } Q_D, \quad u_{B,n'} \to u_{B,\infty} \quad \text{in } Q_B$$

Let us verify that $u_{D,i,\infty} = u_{D,i}(\kappa_\infty, \mu_\infty)$. From (10),

$$\int_\Omega \left[\kappa_{n'} \nabla u_{D,i,n'} \cdot \nabla \overline{v} + \left(\mu_{n'} + \frac{\mathrm{i}\omega}{c_0} \right) u_{D,i,n'} \overline{v} \right] \mathrm{d}x$$

$$+ \int_\Gamma \frac{1}{2A} u_{D,i,n'} \overline{v} \, \mathrm{d}s = \int_\Gamma \frac{1}{2A} p_{D,i} \overline{v} \, \mathrm{d}s \quad \forall v \in V_D \tag{14}$$

Fix an arbitrary v from the complex space $C^\infty(\overline{\Omega})$. Write

$$\int_\Omega (\kappa_{n'} \nabla u_{D,i,n'} \cdot \nabla \overline{v} - \kappa_\infty \nabla u_{D,i,\infty} \cdot \nabla \overline{v}) \, \mathrm{d}x = \int_\Omega (\kappa_{n'} - \kappa_\infty) \nabla u_{D,i,n'} \cdot \nabla \overline{v} \, \mathrm{d}x$$

$$+ \int_\Omega \kappa_\infty \nabla (u_{D,i,n'} - u_{D,i,\infty}) \cdot \nabla \overline{v} \, \mathrm{d}x$$

As $n' \to \infty$, the first integral on the right side approaches zero since $\kappa_{n'} \to \kappa_\infty$ in $L^\infty(\Omega)$ and $\|\nabla u_{D,i,n'}\|_{L^2(\Omega)}$ is uniformly bounded, and the second integral approaches zero since $\kappa_\infty \nabla \overline{v} \in [L^2(\Omega)]^d$ and $u_{D,i,n'} \rightharpoonup u_{D,i,\infty}$ in V_D. Thus,

$$\int_\Omega \kappa_{n'} \nabla u_{D,i,n'} \cdot \nabla \overline{v} \, \mathrm{d}x \to \int_\Omega \kappa_\infty \nabla u_{D,i,\infty} \cdot \nabla \overline{v} \, \mathrm{d}x \quad \text{as } n' \to \infty$$

Write

$$\int_\Omega (\mu_{n'} u_{D,i,n'} - \mu_\infty u_{D,i,\infty}) \overline{v} \, \mathrm{d}x = \int_\Omega (\mu_{n'} - \mu_\infty) u_{D,i,\infty} \overline{v} \, \mathrm{d}x + \int_\Omega \mu_{n'} (u_{D,i,n'} - u_{D,i,\infty}) \overline{v} \, \mathrm{d}x$$

As $n' \to \infty$, the first integral on the right side goes to zero since $\mu_{n'} \rightharpoonup \mu_\infty$ in $L^2(\Omega)$ and $u_{D,i,\infty}\overline{v} \in L^2(\Omega)$, and the second integral goes to zero since $u_{D,i,n'} \to u_{D,i,\infty}$ in $L^2(\Omega)$ and $\|\mu_{n'}\|_{L^2(\Omega)}$ is uniformly bounded. Thus,

$$\int_\Omega \mu_{n'} u_{D,i,n'} \overline{v} \, \mathrm{d}x \to \int_\Omega \mu_\infty u_{D,i,\infty} \overline{v} \, \mathrm{d}x \quad \text{as } n' \to \infty$$

Since $u_{D,i,n'} \to u_{D,i,\infty}$ in $L^2(\Omega)$ and $u_{D,i,n'} \to u_{D,i,\infty}$ in $L^2(\Gamma)$

$$\int_\Omega u_{D,i,n'} \overline{v} \, \mathrm{d}x \to \int_\Omega u_{D,i,\infty} \overline{v} \, \mathrm{d}x$$

$$\int_\Gamma \frac{1}{2A} u_{D,i,n'} \overline{v} \, \mathrm{d}s \to \int_\Gamma \frac{1}{2A} u_{D,i,\infty} \overline{v} \, \mathrm{d}s$$

as $n' \to \infty$. So taking the limit $n' \to \infty$ in (14) for $v \in C^\infty(\overline{\Omega})$, we obtain

$$\int_\Omega \left[\kappa_\infty \nabla u_{D,i,\infty} \cdot \nabla \overline{v} + \left(\mu_\infty + \frac{\mathrm{i}\omega}{c_0} \right) u_{D,i,\infty} \overline{v} \right] \mathrm{d}x + \int_\Gamma \frac{1}{2A} u_{D,i,\infty} \overline{v} \, \mathrm{d}s = \int_\Gamma \frac{1}{2A} p_{D,i} \overline{v} \, \mathrm{d}s$$

Since $C^\infty(\overline{\Omega})$ is dense in V_D, a density argument shows

$$\int_\Omega \left[\kappa_\infty \nabla u_{D,i,\infty} \cdot \nabla \overline{v} + \left(\mu_\infty + \frac{\mathrm{i}\omega}{c_0} \right) u_{D,i,\infty} \overline{v} \right] \mathrm{d}x$$

$$+ \int_\Gamma \frac{1}{2A} u_{D,i,\infty} \overline{v} \, \mathrm{d}s = \int_\Gamma \frac{1}{2A} p_{D,i} \overline{v} \, \mathrm{d}s \quad \forall v \in V_D \tag{15}$$

Thus, $u_{D,i,\infty} = u_{D,i}(\kappa_\infty, \mu_\infty)$.

A similar argument shows that $u_{B,\infty} = u_B(\kappa_\infty, \mu_\infty, p_\infty)$.

Therefore,

$$J_\varepsilon(\kappa_\infty, \mu_\infty, p_\infty) \leqslant \liminf_{n' \to \infty} J_\varepsilon(\kappa_{n'}, \mu_{n'}, p_{n'}) = \alpha$$

i.e. $(\kappa_\infty, \mu_\infty, p_\infty) \in Q_{\mathrm{ad}}$ is a solution of the problem (13). $\qquad \square$

We comment that the condition $\varepsilon_p > 0$ is natural in practical simulations as the corresponding term plays a regularization role.

The next result provides a necessary condition for a solution of the problem (13).

Proposition 2.2
Let $(\kappa_0, \mu_0, p_0) \in Q_{\mathrm{ad}}$ be a solution of the problem (13) and denote $u_{D,i,0} = u_{D,i}(\kappa_0, \mu_0)$ and $u_{B,0} = u_B(\kappa_0, \mu_0, p_0)$. Then

$$\sum_{i=1}^I \mathrm{Re}(u_{D,i,0} - g_{D,i}, w_{D,i,0})_{L^2(\Gamma_{D,i})} + (u_{B,0} - g_B, w_{B,0})_{L^2(\Gamma_B)} + \varepsilon_\kappa(\kappa_0, \kappa - \kappa_0)_{L^2(\Omega)}$$

$$+ \varepsilon_\mu(\mu_0, \mu - \mu_0)_{L^2(\Omega)} + \varepsilon_p(p_0, p - p_0)_{L^2(\Omega_B)} \geqslant 0 \quad \forall (\kappa, \mu, p) \in Q_{\mathrm{ad}} \tag{16}$$

where $w_{D,i,0} = w_{D,i,0}(\kappa - \kappa_0, \mu - \mu_0) \in V_D$ is the solution of the BVP

$$\int_\Omega \left[\kappa_0 \nabla w_{D,i,0} \cdot \nabla \overline{v} + \left(\mu_0 + \frac{i\omega}{c_0} \right) w_{D,i,0} \overline{v} \right] dx + \int_\Gamma \frac{1}{2A} w_{D,i,0} \overline{v} \, ds$$

$$= - \int_\Omega [(\kappa - \kappa_0) \nabla u_{D,i,0} \cdot \nabla \overline{v} + (\mu - \mu_0) u_{D,i,0} \overline{v}] \, dx \quad \forall v \in V_D \tag{17}$$

whereas $w_{B,0} = w_{B,0}(\kappa - \kappa_0, \mu - \mu_0, p - p_0) \in V_B$ is the solution of the BVP

$$\int_\Omega (\kappa_0 \nabla w_{B,0} \cdot \nabla v + \mu_0 w_{B,0} v) \, dx + \int_\Gamma \frac{1}{2A} w_{B,0} v \, ds$$

$$= \int_{\Omega_B} (p - p_0) v \, dx - \int_\Omega [(\kappa - \kappa_0) \nabla u_{B,0} \cdot \nabla v + (\mu - \mu_0) u_{B,0} v] \, dx \quad \forall v \in V_B \tag{18}$$

Proof
Let $t \in [0, 1]$ be a real variable. For any $(\kappa, \mu, p) \in Q_{\text{ad}}$, write

$$\kappa_t = \kappa_0 + t(\kappa - \kappa_0)$$

$$\mu_t = \mu_0 + t(\mu - \mu_0)$$

$$p_t = p_0 + t(p - p_0)$$

Define $u_{D,i,t} \in V_D$ and $u_{B,t} \in V_B$ to be the solutions of the following boundary value problems:

$$\int_\Omega \left[\kappa_t \nabla u_{D,i,t} \cdot \nabla \overline{v} + \left(\mu_t + \frac{i\omega}{c_0} \right) u_{D,i,t} \overline{v} \right] dx + \int_\Gamma \frac{1}{2A} u_{D,i,t} \overline{v} \, ds$$

$$= \int_\Gamma \frac{1}{2A} p_{D,i} \overline{v} \, ds \quad \forall v \in V_D \tag{19}$$

$$\int_\Omega [\kappa_t \nabla u_{B,t} \cdot \nabla v + \mu_t u_{B,t} v] \, dx + \int_\Gamma \frac{1}{2A} u_{B,t} v \, ds = \int_{\Omega_B} p_t v \, dx \quad \forall v \in V_B \tag{20}$$

Consider the function

$$g(t) = \sum_{i=1}^I \|u_{D,i,t} - g_{D,i}\|_{L^2(\Gamma_{D,i})}^2 + \|u_{B,t} - g_B\|_{L^2(\Gamma_B)}^2 + \varepsilon_\kappa \|\kappa_t\|_{L^2(\Omega)}^2 + \varepsilon_\mu \|\mu_t\|_{L^2(\Omega)}^2 + \varepsilon_p \|p_t\|_{L^2(\Omega_B)}^2$$

for $t \in [0, 1]$. Then $g(t)$ has its minimum at $t = 0$ for $t \in [0, 1]$, and so

$$g'(0+) \geqslant 0$$

Now

$$\frac{1}{2} g'(t) = \sum_{i=1}^I \text{Re} \left(u_{D,i,t} - g_{D,i}, \frac{\partial u_{D,i,t}}{\partial t} \right)_{L^2(\Gamma_{D,i})} + \left(u_{B,t} - g_B, \frac{\partial u_{B,t}}{\partial t} \right)_{L^2(\Gamma_B)}$$

$$+ \varepsilon_\kappa (\kappa_t, \kappa - \kappa_0)_{L^2(\Omega)} + \varepsilon_\mu (\mu_t, \mu - \mu_0)_{L^2(\Omega)} + \varepsilon_p (p_t, p - p_0)_{L^2(\Omega_B)}$$

Differentiate (19) with respect to t to obtain

$$\int_\Omega \left[\kappa_t \nabla \frac{\partial u_{D,i,t}}{\partial t} \cdot \nabla \overline{v} + \left(\mu_t + \frac{\mathrm{i}\omega}{c_0} \right) \frac{\partial u_{D,i,t}}{\partial t} \overline{v} \right] \mathrm{d}x + \int_\Gamma \frac{1}{2A} \frac{\partial u_{D,i,t}}{\partial t} \overline{v} \, \mathrm{d}s$$

$$= -\int_\Omega [(\kappa - \kappa_0) \nabla u_{D,i,t} \cdot \nabla \overline{v} + (\mu - \mu_0) u_{D,i,t} \overline{v}] \, \mathrm{d}x \quad \forall v \in V_D \qquad (21)$$

Obviously, $u_{D,i,t} : t \in [0,1] \to V_D$ is continuous as a function of t. So $u_{D,i,t} \to u_{D,i,0}$ in V_D as $t \to 0+$. Let $t \to 0+$ in (21) to obtain (17) for

$$w_{D,i,0} = \lim_{t \to 0+} \frac{\partial u_{D,i,t}}{\partial t}$$

Similarly, we can derive the boundary value problem (18) for

$$w_{B,0} = \lim_{t \to 0+} \frac{\partial u_{B,t}}{\partial t}$$

Thus,

$$\frac{1}{2} g'(0+) = \sum_{i=1}^I \mathrm{Re}(u_{D,i,0} - g_{D,i}, w_{D,i,0})_{L^2(\Gamma_{D,i})} + (u_{B,0} - g_B, w_{B,0})_{L^2(\Gamma_B)}$$

$$+ \varepsilon_\kappa(\kappa_0, \kappa - \kappa_0)_{L^2(\Omega)} + \varepsilon_\mu(\mu_0, \mu - \mu_0)_{L^2(\Omega)} + \varepsilon_p(p_0, p - p_0)_{L^2(\Omega_B)} \geqslant 0$$

i.e. (16) holds.   □

The proposition gives a necessary condition for a solution of the problem (13). The result may be useful in studying solution properties.

We have addressed the existence of a solution to Problem (13) in Theorem 2.1. Solution uniqueness is an issue worth further exploring for both Problem (13) and its non-regularized limit with $\varepsilon_\kappa = \varepsilon_\mu = \varepsilon_p = 0$. In the case of a pure BLT problem, a solution uniqueness result for the counterpart of Problem (13) with $\varepsilon_p > 0$ is proved in [3]. Moreover, it is shown there that as $\varepsilon_p \to 0$, we will recover the minimal norm solution of the BLT problem without regularization. In the case of a pure DOT problem, some solution uniqueness results are found in [9, 10] under the assumption of availability of complete knowledge of the so-called Dirichlet-to-Neumann operator. In practice, the optical parameters are usually assumed to be piecewise constants. For such situation, some theoretical results on solution uniqueness can be found in the literature, e.g. [11, 12]. However, the results are generally difficult to use for applications. In the case of piecewise constant optical parameters, solution uniqueness is likely guaranteed with several sets of measurement data. Below, we illustrate this by considering a simple 1D example with constant parameters. The example is to determine two positive constants κ and μ such that

$$-\kappa u'' + \mu u = 0 \quad \text{in } (0,1)$$

$$u(0) = f_0, \quad u(1) = f_1$$

$$-\kappa u'(0) = g_0, \quad \kappa u'(1) = g_1$$

for given values f_0, f_1, g_0, and g_1 with $f_1 g_0 \neq f_0 g_1$. After some calculations, it can be shown that

$$(f_1 g_0 - f_0 g_1) \cosh(\sqrt{\mu/\kappa}) = f_0 g_0 - f_1 g_1 \tag{22}$$

and

$$\sqrt{\kappa \mu} = -\frac{g_0 \sinh(\sqrt{\mu/\kappa})}{f_1 - f_0 \cosh(\sqrt{\mu/\kappa})} \tag{23}$$

Obviously, if a solution (κ, μ) exists, then it is uniquely determined by (22) and (23).

3. NUMERICAL APPROXIMATIONS

In this section, we consider numerical solutions of the problem (13). Our discussion can be given for the general sets Q_κ of (7) and Q_μ of (8) for the optical parameters, following the same kind of arguments presented below, at the expense of more complicated notations and the mathematical expressions. In order to focus on the essential parts of the arguments, in this section, we restrict our discussion to the situation where the optical parameters are piecewise constants.

Let $\{\mathcal{T}_h\}$ (h: meshsize) be a regular family of finite element partitions of $\overline{\Omega}$ such that each element at the boundary Γ has at most one non-straight face (for a three-dimensional domain) or side (for a two-dimensional domain). For each triangulation, $\mathcal{T}_h = \{K\}$, let $V_D^h \subset V_D$ and $V_B^h \subset V_B$ be the corresponding linear element spaces. Let $\{\mathcal{T}_{H, \Omega_B}\}$ (H: meshsize) be a regular family of finite element partitions of $\overline{\Omega_B}$ such that each element at the boundary $\partial \Omega_B$ has at most one non-straight face (for a three-dimensional domain) or side (for a two-dimensional domain). The introduction of the second family of partitions $\{\mathcal{T}_{H, \Omega_B}\}$ is for flexibility, and it is allowed to be the restriction of the family $\{\mathcal{T}_h\}$ on the set Ω_B if the boundary $\partial \Omega_B$ is the union of some sides for any partition $\mathcal{T}_h$ under consideration. Let Q_p^H be the piecewise constant finite element subset approximating Q_p. Then Q_p^H is non-empty, closed, and convex, and we have the property

$$\forall q \in Q_p, \ \exists q^H \in Q_p^H \quad \text{such that } \|q^H - q\|_{L^2(\Omega_B)} \to 0 \ \text{as } H \to 0$$

Indeed, we may simply take q^H to be the piecewise average of q over $\mathcal{T}_{H, \Omega_B}$. Denote $u_{D,i}^h = u_{D,i}^h(\kappa, \mu) \in V_D^h$ for the solution of the problem

$$\int_\Omega \left[\kappa \nabla u_{D,i}^h \cdot \nabla \overline{v^h} + \left(\mu + \frac{\mathrm{i}\omega}{c_0} \right) u_{D,i}^h \overline{v^h} \right] \mathrm{d}x + \int_\Gamma \frac{1}{2A} u_{D,i}^h \overline{v^h} \, \mathrm{d}s = \int_\Gamma \frac{1}{2A} p_{D,i} \overline{v^h} \, \mathrm{d}s \quad \forall v^h \in V_D^h \tag{24}$$

Also, let $u_B^{hH} = u_B^h(\kappa, \mu, p^H) \in V_B^h$ be the solution of the problem

$$\int_\Omega (\kappa \nabla u_B^{hH} \cdot \nabla v^h + \mu u_B^{hH} v^h) \, \mathrm{d}x + \int_\Gamma \frac{1}{2A} u_B^{hH} v^h \, \mathrm{d}s = \int_{\Omega_B} p^H v^h \, \mathrm{d}x \quad \forall v^h \in V_B^h \tag{25}$$

By the Lax–Milgram Lemma, both $u_{D,i}^h$ and u_B^{hH} are uniquely defined. As an approximation of the functional (12), we let

$$J_\varepsilon^{hH}(\kappa, \mu, p^H) = \frac{1}{2} \sum_{i=1}^{I} \|u_{D,i}^h(\kappa, \mu) - g_{D,i}\|_{L^2(\Gamma_{D,i})}^2 + \frac{1}{2} \|u_B^{hH}(\kappa, \mu, p^H) - g_B\|_{L^2(\Gamma_B)}^2$$

$$+ \frac{\varepsilon_\kappa}{2} \|\kappa\|_{L^2(\Omega)}^2 + \frac{\varepsilon_\mu}{2} \|\mu\|_{L^2(\Omega)}^2 + \frac{\varepsilon_p}{2} \|p^H\|_{L^2(\Omega_B)}^2 \tag{26}$$

We then introduce the following discretization of the problem (13):

$$\inf\{J_\varepsilon^{hH}(\kappa, \mu, p^H) \mid (\kappa, \mu, p^H) \in Q_{\mathrm{ad}}^H\} \tag{27}$$

where $Q_{\mathrm{ad}}^H = Q_\kappa \times Q_\mu \times Q_p^H$ is the admissible set for the discretized problem.

Like for the problem (13), under the assumption of Theorem 2.1, there is a solution to the discrete problem (27). Let us show the following convergence result of the numerical method.

Theorem 3.1
(a) Any sequence of discrete solutions of the problem (27) corresponding to a sequence of meshsizes contains a subsequence $\{(\kappa^{hH}, \mu^{hH}, p^{hH})\}_{h,H}$ and a solution $(\kappa, \mu, p) \in Q_{\mathrm{ad}}$ of the problem (13) such that

$$\kappa^{hH} \to \kappa \text{ and } \mu^{hH} \to \mu \quad \text{in } L^\infty(\Omega), \quad p^{hH} \to p \quad \text{in } L^2(\Omega_B) \text{ as } h, H \to 0 \tag{28}$$

(b) Any limiting point (κ, μ, p) of a sequence $\{(\kappa^{hH}, \mu^{hH}, p^{hH})\}_{h,H}$ of discrete solutions defined by the problem (27), in the sense of (28), is a solution of the problem (13).

(c) Denote by α^{hH} the infimum value of (27). Then

$$\alpha^{hH} \to \alpha \quad \text{as } h, H \to 0$$

Proof
Let $(\kappa_\infty, \mu_\infty, p_\infty) \in Q_{\mathrm{ad}}$ be a solution of (13). Note that $u_{D,i,\infty} = u_{D,i}(\kappa_\infty, \mu_\infty) \in V_D$ satisfies (15). Denote $u_{D,i,\infty}^h = u_{D,i}^h(\kappa_\infty, \mu_\infty) \in V_D^h$. Then by (24), for any $v^h \in V_D^h$

$$\int_\Omega \left[\kappa_\infty \nabla u_{D,i,\infty}^h \cdot \nabla \overline{v^h} + \left(\mu_\infty + \frac{\mathrm{i}\omega}{c_0} \right) u_{D,i,\infty}^h \overline{v^h} \right] \mathrm{d}x + \int_\Gamma \frac{1}{2A} u_{D,i,\infty}^h \overline{v^h} \mathrm{d}s = \int_\Gamma \frac{1}{2A} p_{D,i} \overline{v^h} \mathrm{d}s$$

By Cea's inequality we have

$$\|u_{D,i,\infty} - u_{D,i,\infty}^h\|_{V_D} \leqslant c \inf_{v^h \in V_D^h} \|u_{D,i,\infty} - v^h\|_{V_D} \to 0 \quad \text{as } h \to 0$$

Similarly, $u_{B,\infty} = u_B(\kappa_\infty, \mu_\infty, p_\infty) \in V_B$ is the solution of the BVP

$$\int_\Omega (\kappa_\infty \nabla u_{B,\infty} \cdot \nabla v + \mu_\infty u_{B,\infty} v) \mathrm{d}x + \int_\Gamma \frac{1}{2A} u_{B,\infty} v \mathrm{d}s = \int_{\Omega_B} p_\infty v \mathrm{d}x \quad \forall v \in V_B \tag{29}$$

Choose $p_\infty^H \in Q_p^H$ such that

$$p_\infty^H \to p_\infty \quad \text{in } L^2(\Omega_0) \text{ as } H \to 0 \tag{30}$$

By (25), $u_{B,\infty}^{hH} \in V_B^h$ is the discrete solution defined by the relation

$$\int_\Omega (\kappa_\infty \nabla u_{B,\infty}^{hH} \cdot \nabla v^h + \mu_\infty u_{B,\infty}^{hH} v^h)\,dx + \int_\Gamma \frac{1}{2A} u_{B,\infty}^{hH} v^h \,ds = \int_{\Omega_B} p_\infty^H v^h \,dx \quad \forall v^h \in V_B^h$$

Subtract this relation from (29) to obtain

$$\int_\Omega [\kappa_\infty \nabla (u_{B,\infty} - u_{B,\infty}^{hH}) \cdot \nabla v^h + \mu_\infty (u_{B,\infty} - u_{B,\infty}^{hH}) v^h]\,dx + \int_\Gamma \frac{1}{2A}(u_{B,\infty} - u_{B,\infty}^{hH}) v^h \,ds$$

$$= \int_{\Omega_B} (p_\infty - p_\infty^H) v^h \,dx \quad \forall v^h \in V_B^h$$

Using this, we obtain

$$\|u_{B,\infty} - u_{B,\infty}^{hH}\|_{V_B} \leqslant c \left[\inf_{v^h \in V_B^h} \|u_{B,\infty} - v^h\|_{V_B} + \|p_\infty - p_\infty^H\|_{L^2(\Omega_B)} \right] \to 0 \quad \text{as } h, H \to 0$$

Since $\alpha^{hH} \leqslant J_\varepsilon^{hH}(\kappa_\infty, \mu_\infty, p_\infty^H)$, we have

$$\limsup_{h, H \to 0} \alpha^{hH} \leqslant \lim_{h, H \to 0} J_\varepsilon^{hH}(\kappa_\infty, \mu_\infty, p_\infty^H) = \alpha \tag{31}$$

Consider any sequence $\{(\kappa^{hH}, \mu^{hH}, p^{hH})\}_{h,H}$ of solutions of the problem (27). Then there is a subsequence, still denoted by $\{(\kappa^{hH}, \mu^{hH}, p^{hH})\}_{h,H}$, such that for some $\kappa \in Q_\kappa$, $\mu \in Q_\mu$, and $p \in Q_p$

$$\kappa^{hH} \to \kappa \text{ and } \mu^{hH} \to \mu \quad \text{in } L^\infty(\Omega), \quad p^{hH} \rightharpoonup p \quad \text{in } L^2(\Omega_B) \text{ as } h, H \to 0 \tag{32}$$

Let us show that

$$u_{D,i}^{hH} = u_{D,i}^h(\kappa^{hH}, \mu^{hH}) \rightharpoonup u_{D,i}(\kappa, \mu) \quad \text{in } V_D \text{ as } h, H \to 0$$

First, by (24), it can be shown that $\|u_{D,i}^{hH}\|_{V_D}$ is uniformly bounded, independent of h and H. So there exists a subsequence of $\{u_{D,i}^{hH}\}_{h,H}$, still denoted by $\{u_{D,i}^{hH}\}_{h,H}$, and $u_{D,i} \in V_D$ such that $u_{D,i}^{hH} \rightharpoonup u_{D,i}$ in V_D. Taking $h, H \to 0$ along this subsequence in (24) with $\kappa = \kappa^{hH}$ and $\mu = \mu^{hH}$ to get

$$\int_\Omega \left[\kappa \nabla u_{D,i} \cdot \nabla \overline{v} + \left(\mu + \frac{i\omega}{c_0} \right) u_{D,i} \overline{v} \right] dx + \int_\Gamma \frac{1}{2A} u_{D,i} \overline{v} \,ds = \int_\Gamma \frac{1}{2A} p_{D,i} \overline{v} \,ds \quad \forall v \in V_D$$

i.e. the limit $u_{D,i} = u_{D,i}(\kappa, \mu)$. Since the limit $u_{D,i}$ is unique, the entire family converges: $u_{D,i}^{hH} \rightharpoonup u_{D,i}$ in V_D as $h, H \to 0$. A consequence of this is $u_{D,i}^h(\kappa^{hH}, \mu^{hH}) \to u_{D,i}(\kappa, \mu)$ in Q_D. Similarly, $u_B^{hH} = u_B^h(\kappa^{hH}, \mu^{hH}, p^{hH}) \rightharpoonup u_B(\kappa, \mu, p)$ in V_B and $u_B^{hH} \to u_B(\kappa, \mu, p)$ in Q_B. Hence,

$$J_\varepsilon(\kappa, \mu, p) \leqslant \liminf_{h, H \to 0} J_\varepsilon^{hH}(\kappa^{hH}, \mu^{hH}, p^{hH}) \tag{33}$$

and so

$$\liminf_{h, H \to 0} \alpha^{hH} \geqslant \alpha \tag{34}$$

Combining (31) and (34), we see that the statement (c) holds. From (33), we deduce that (κ, μ, p) is a solution of the problem (13). Moreover,

$$\lim_{h, H \to 0} J_\varepsilon^{hH}(\kappa^{hH}, \mu^{hH}, p^{hH}) = J_\varepsilon(\kappa, \mu, p)$$

and therefore,

$$\lim_{h, H \to 0} \|p^{hH}\|_{L^2(\Omega_B)} = \|p\|_{L^2(\Omega_B)}$$

This relation and (32) together lead to (28) ([6]). Hence, the statement (a) is valid. The above argument also shows that the statement (b) is valid.   □

The theorem states that as the finite element meshsizes go to zero, we have convergence of numerical solutions and convergence of the minimal discrete energy to the minimal energy.

4. NUMERICAL EXAMPLES

We report numerical results on two examples.

First, we consider a two-dimensional test problem. In this example, we take $\omega = 0$, that is both DOT and BLT are performed in continuous wave domain. Let $\Omega = (0, 1) \times (0, 1)$ divide it into two sub-regions: $\Omega_1 = (0, 0.5) \times (0, 1)$ and $\Omega_2 = (0.5, 1) \times (0, 1)$. In each region Ω_m, $m = 1, 2$, the values of the optical parameters κ and μ are assumed to be constant. The exact values of κ and μ are taken to be

$$\kappa = \begin{cases} 0.3268 & \text{in } \Omega_1 \\ 0.1916 & \text{in } \Omega_2 \end{cases} \qquad \mu = \begin{cases} 0.02 & \text{in } \Omega_1 \\ 0.14 & \text{in } \Omega_2 \end{cases}$$

We specify the ranges for the optical parameters by $\kappa \in [0.01, 2]$ and $\mu \in [0.001, 1.2]$. We take six different intensities of the source p_D on the boundary Γ. We assume that each $p_{D,i}$, $1 \leqslant i \leqslant 6$, has a constant value on Γ.

$$p_{D,1} = 3 \qquad \text{on } \Gamma$$
$$p_{D,2} = 4 \qquad \text{on } \Gamma$$
$$p_{D,3} = 6 \qquad \text{on } \Gamma$$
$$p_{D,4} = 7 \qquad \text{on } \Gamma$$
$$p_{D,5} = 8 \qquad \text{on } \Gamma$$
$$p_{D,6} = 10 \quad \text{on } \Gamma$$

The source function p_B is assumed to be piecewise constant. The source is placed in the permissible region $\overline{\Omega_0} = [0.25, 0.375] \times [0.375, 0.625]$, which is divided into four uniform triangular elements. In each element, the value of source function p_B is taken to be 10. In this example, we choose $A = 1$.

We use linear elements on uniform triangular partitions of the domain Ω. The uniform meshes are obtained by dividing the interval $[0, 1]$ into $1/h$ equal parts in both x and y directions. We start with an initial mesh with $h = \frac{1}{8}$ and then successively halve h to obtain more refined meshes.

The numerical solutions of the boundary value problems (10) and (11) computed using the exact values of κ, μ, and p_B, and on the mesh with mesh size $h = \frac{1}{512}$ are taken as the true solutions. These solutions are then used to obtain the measured quantity $g_{D,i}$, $1 \leqslant i \leqslant 4$, on $\Gamma_D = \Gamma$ and g_B on $\Gamma_B = \Gamma$.

The numerical solutions of problem (13) are then computed using these values of $g_{D,i}$, $1 \leqslant i \leqslant 4$, and g_B on the meshes with mesh size $h = \frac{1}{8}$, $\frac{1}{16}$, $\frac{1}{32}$, $\frac{1}{64}$, and regularization parameters $\varepsilon_\kappa = 10^{-5}$, $\varepsilon_\mu = 10^{-5}$ and $\varepsilon_p = 10^{-5}$.

Tables I–III give the computed values of κ^h, μ^h, and p_B^h for various values of h and using just one set of measurement data corresponding to $p_{D,2}$. The norm of the error between the true and computed values of κ, μ, and p_B using various number of measurement data sets for g_D and mesh size h is given in Tables IV–VI. Errors of numerical solutions given in Tables I–III are shown graphically in Figures 1–3.

Table I. Numerical results on parameter κ.

Subdomain	Ω_1	Ω_2
$\kappa^h, h = \frac{1}{8}$	0.3434	0.1993
$\kappa^h, h = \frac{1}{16}$	0.3320	0.1934
$\kappa^h, h = \frac{1}{32}$	0.3282	0.1919
$\kappa^h, h = \frac{1}{64}$	0.3272	0.1917
κ	0.3268	0.1916

Table II. Numerical results on parameter μ.

Subdomain	Ω_1	Ω_2
$\mu^h, h = \frac{1}{8}$	0.019374	0.139657
$\mu^h, h = \frac{1}{16}$	0.019763	0.139995
$\mu^h, h = \frac{1}{32}$	0.019926	0.140013
$\mu^h, h = \frac{1}{64}$	0.019978	0.140008
μ	0.02	0.14

Table III. Numerical results on source function p_B.

Element	1	2	3	4
$p_B^h, h = \frac{1}{8}$	9.6222	10.0785	9.6363	10.3618
$p_B^h, h = \frac{1}{16}$	9.8517	10.0743	9.7969	10.1454
$p_B^h, h = \frac{1}{32}$	9.9423	10.0665	9.8285	10.1010
$p_B^h, h = \frac{1}{64}$	10.0035	10.0266	9.8371	10.1035
p_B	10.0	10.0	10.0	10.0

Table IV. $\|\kappa - \kappa^h\|_{L^2(\Omega)}$.

No. of data sets	$h = \frac{1}{8}$	$h = \frac{1}{16}$	$h = \frac{1}{32}$	$h = \frac{1}{64}$
1	2.4336×10^{-2}	6.9232×10^{-3}	1.7439×10^{-3}	4.6583×10^{-4}
2	2.4427×10^{-2}	6.9181×10^{-3}	1.7907×10^{-3}	4.4289×10^{-4}
4	2.4446×10^{-2}	7.1579×10^{-3}	1.8736×10^{-3}	4.8085×10^{-4}
6	2.4440×10^{-2}	7.1725×10^{-3}	1.8763×10^{-3}	4.8678×10^{-4}

Table V. $\|\mu - \mu^h\|_{L^2(\Omega)}$.

No. of data sets	$h = \frac{1}{8}$	$h = \frac{1}{16}$	$h = \frac{1}{32}$	$h = \frac{1}{64}$
1	9.6949×10^{-4}	2.4187×10^{-4}	6.0002×10^{-5}	1.4517×10^{-5}
2	9.7234×10^{-4}	2.4265×10^{-4}	5.9840×10^{-5}	1.4655×10^{-5}
4	9.7899×10^{-4}	2.4443×10^{-4}	5.9761×10^{-5}	1.4501×10^{-5}
6	9.7978×10^{-4}	2.4470×10^{-4}	5.9712×10^{-5}	1.4243×10^{-5}

Table VI. $\|p_B - p_B^h\|_{L^2(\Omega_0)}$.

No. of data sets	$h = \frac{1}{8}$	$h = \frac{1}{16}$	$h = \frac{1}{32}$	$h = \frac{1}{64}$
1	5.6736×10^{-2}	2.6500×10^{-2}	1.9238×10^{-2}	1.7225×10^{-2}
2	5.7494×10^{-2}	3.0657×10^{-2}	2.2942×10^{-2}	1.8501×10^{-2}
4	6.6857×10^{-2}	3.7110×10^{-2}	2.1366×10^{-2}	1.4309×10^{-2}
6	6.8125×10^{-2}	3.4272×10^{-2}	2.0590×10^{-2}	2.1809×10^{-2}

To demonstrate the feasibility of the proposed numerical reconstruction method, in the second example, we consider a cylindrical numerical phantom of radius 10 mm and height 20 mm, which includes two regions Ω_1 and Ω_2, as shown in Figures 4 and 5. A spherical light source of radius of 0.6 mm with power of 1.16 nano-Watts is located at $(-3, -1, 10)$ in region Ω_2. The optical parameters (μ, D) of the two regions are assigned as $(0.06 \, \text{mm}^{-1}, 0.42735 \, \text{mm})$, and $(0.12 \, \text{mm}^{-1}, 0.24331 \, \text{mm})$ to simulate heterogeneous medium. The finite element method with linear elements is applied to solve the boundary value problems. The phantom is discretized into 88 360 tetrahedral elements with 16 316 nodes. There are 3301 boundary nodes and we use them to record photon flux density on the boundary. In practice, the measurement modality can be realized using non-contact imaging using highly sensitive CCD camera. For the parameter A, we use, as usual, the formula

$$A = (1 + R)/(1 - R)$$

with a directionally varying refraction parameter R computed by

$$R = -1.4399\eta^{-2} + 0.7099\eta^{-1} + 0.6681 + 0.0636\eta$$
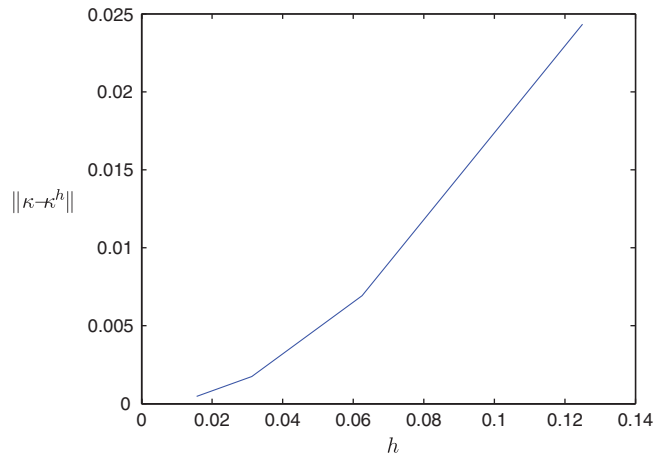
Figure 1. Graph of the error $\|\kappa - \kappa^h\|_{L^2(\Omega)}$.
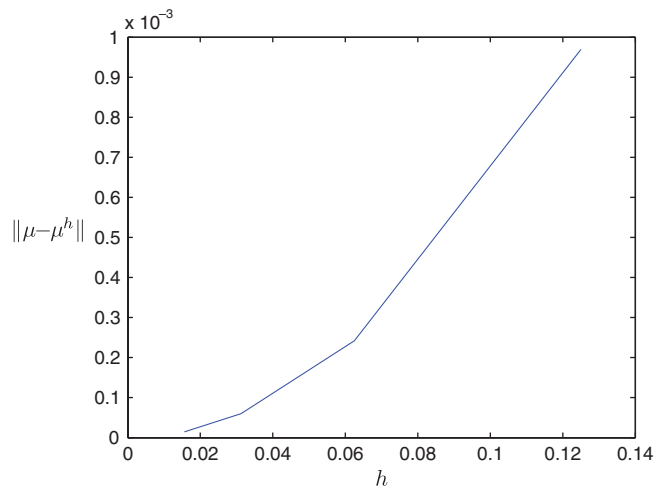
Figure 2. Graph of the error $\|\mu - \mu^h\|_{L^2(\Omega)}$.

In this example, we take the refractive index $\eta = 1.37$. The measured data on the boundary are generated from the solution of the BVP (4)–(5), corrupted by 5% Gaussian noise, as shown in Figure 6.

Four point sources of 10 nano-Watts with a modulation frequency of 100 MHz located at $(0, -10, 10)$, $(0, 10, 11)$, $(10, 0, 12)$, and $(-10, 0, 13)$ on the boundary are employed to excite the phantom, respectively, and the virtual detectors collect photon flux density on the boundary of the phantom to get four sets of measurement data $g_{D,i}$, $1 \leqslant i \leqslant 4$, respectively, based on boundary value problem (1)–(3). The measurement data $g_{D,i}$, $1 \leqslant i \leqslant 4$ are corrupted by 5% Gaussian noise. We
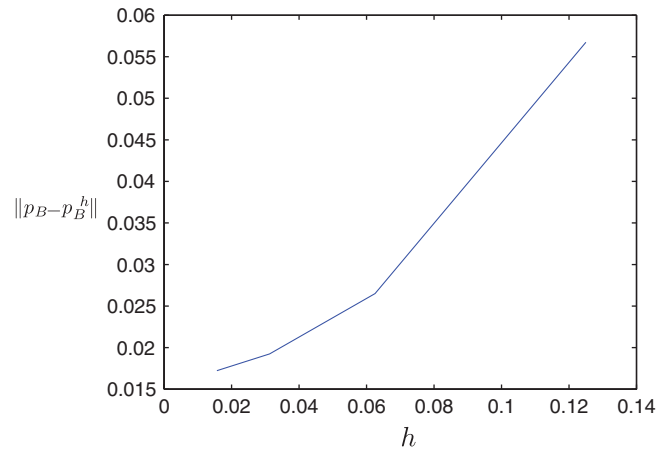
Figure 3. Graph of the error $\|p_B - p_B^h\|_{L^2(\Omega)}$.
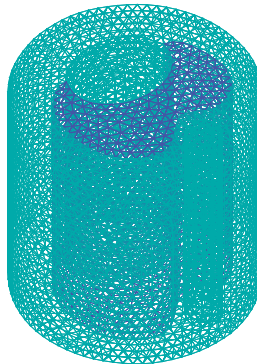
Figure 4. Geometry of phantom: three-dimensional geometrical view.

have

$$p_{D,1}(x, y, z) = 10\delta(x)\delta(y+10)\delta(z-10)\,e^{-i\beta}$$

$$p_{D,2}(x, y, z) = 10\delta(x)\delta(y-10)\delta(z-11)\,e^{-i\beta}$$

$$p_{D,3}(x, y, z) = 10\delta(x-10)\delta(y)\delta(z-12)\,e^{-i\beta}$$

$$p_{D,4}(x, y, z) = 10\delta(x+10)\delta(y)\delta(z-13)\,e^{-i\beta}$$

where $\beta = 2\pi \times \text{frequency}/(\text{light speed}) = (2/3)\pi \times 10^{-3}$. Note that with the four point sources on the boundary, the right-hand side of the finite element system (24) is interpreted to be $(1/2A) \times 10 \times v^h$ evaluated at the points $(0, -10, 10)$, $(0, 10, 11)$, $(10, 0, 12)$, and $(-10, 0, 13)$, respectively. With these point sources, the weak formulation (10) for the BVP (1)–(2) is not well defined.
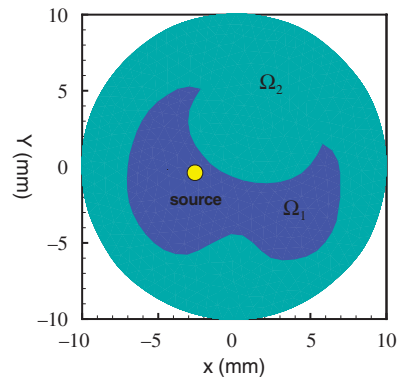
Figure 5. Geometry of phantom: two-dimensional geometrical view.
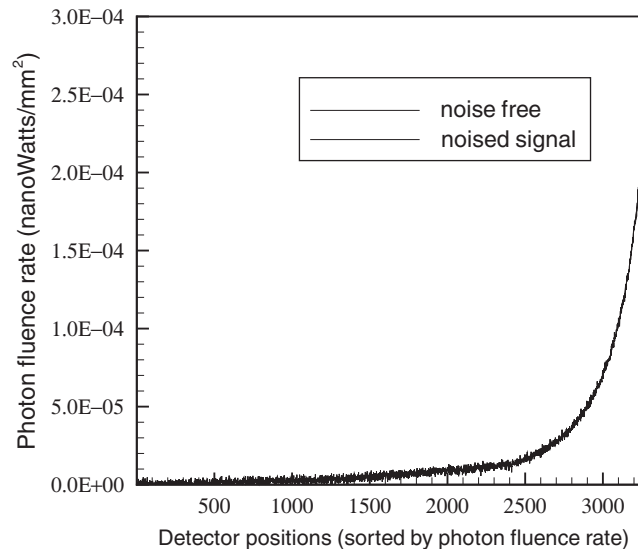
Figure 6. Measurement data.

However, we may interpret the solution of the system (24) as a finite element approximation of the weak solution of the BVP (1)–(2) with a smoothed source function $\tilde{p}_{D,i}$.

The source permissible region Ω_0 is set to be a ball with radius 1.0 mm and centered at $(-3, -1, 10)$. The admissible ranges of optical parameters are chosen as

$$\mu_1 \in [0.03, 0.12], \quad \mu_2 \in [0.06, 0.24], \quad D_1 \in [0.21, 0.85], \quad D_2 \in [0.12, 0.48]$$

The reconstruction problem is of the form (27) in identifying the optical parameters and light source distribution. The regularization parameters are $\varepsilon_\kappa = 10^{-5}$, $\varepsilon_\mu = 10^{-5}$, and $\varepsilon_p = 10^{-8}$. Matlab Optimization Toolbox is used to solve the optimization problem (27). The reconstructed results of

optical parameters and light source power are in good agreement with true values. The reconstructed absorption coefficients of the two regions are 0.1265 and 0.0593, respectively. The relative errors are 5.4, and 1.2% for the regions Ω_1 and Ω_2, respectively. The reconstructed diffusion coefficients are 0.2457 and 0.4263, respectively. The relative errors are 1 and 0.3% for the regions Ω_1 and Ω_2, respectively. The relative error of the reconstructed total light source power is 20%.

For comparison, we also report numerical results by using just one excitation light source $p_{D,1}(x, y, z)$ and the corresponding measurement data $g_{D,1}$ on the boundary. The reconstructed absorption coefficients of the two regions are 0.1632 and 0.0598, respectively. The relative errors are 36, and 0.3% for the regions Ω_1 and Ω_2, respectively. The reconstructed diffusion coefficients are 0.1508 and 0.4270, respectively. The relative errors are 38 and 0.1% for the regions Ω_1 and Ω_2, respectively. The relative error of the reconstructed total light source power is 25%.

REFERENCES

1. Gibson AP, Hebden JC, Arridge SR. Recent advances in diffuse optical imaging. *Physics in Medicine and Biology* 2005; **50**:R1–R43.
2. Wang G, Li Y, Jiang M. Uniqueness theorems in bioluminescence tomography. *Medical Physics* 2004; **31**: 2289–2299.
3. Han W, Cong WX, Wang G. Mathematical theory and numerical analysis of bioluminescence tomography. *Inverse Problems* 2006; **22**:1659–1675.
4. Han W, Cong WX, Wang G. Mathematical study and numerical simulation of multispectral bioluminescence tomography. *International Journal of Biomedical Imaging* 2006; **2006**:10. Article ID 54390. DOI: 10.1155/IJBI/2006/54390.
5. Han W, Wang G. Theoretical and numerical analysis on multispectral bioluminescence tomography. *IMA Journal of Applied Mathematics* 2007; **72**:67–85.
6. Atkinson K, Han W. *Theoretical Numerical Analysis*: *A Functional Analysis Framework* (2nd edn). Springer: New York, 2005.
7. Evans LC. *Partial Differential Equations*. American Mathematical Society: Providence, RI, 1998.
8. Dautray R, Lions JL. *Mathematical Analysis and Numerical Methods for Science and Technology*, vol. 2. Springer: Berlin, Heidelberg, 1988.
9. Arridge SR. Optical tomography in medical imaging. *Inverse Problems* 1999; **15**:R41–R93.
10. Khan T, Thomas A, Yoon J-R. On uniqueness in refractive index optical tomography. *Inverse Problems* 2006; **22**:L1–L5.
11. Kohn R, Vogelius M. Determining conductivity by boundary measurements interior results, vol. II. *Communications on Pure and Applied Mathematics* 1985; **38**:643–667.
12. Druskin V. On the uniqueness of inverse problems from incomplete boundary data. *SIAM Journal on Applied Mathematics* 1998; **58**:1591–1603.